Evaluation of behavior and strength of prestressed concrete deep beams using nonlinear analysis

T.H. Kim[1], J.H. Cheon[2] and H.M. Shin*[2]

[1]*Construction Technology R&D Center, Samsung C&T Corporation, 1321-20 Seocho2-dong, Seocho-gu, Seoul 137-956, Korea*
[2]*Department of Civil and Environmental Engineering, Sungkyunkwan University, 300 Cheoncheon-dong, Jangan-gu, Suwon-si, Gyeonggi-do 440-746, Korea*

(Received October 17, 2010, Revised June 24, 2011, Accepted June 28, 2011)

Abstract. The purpose of this study is to evaluate the behavior and strength of prestressed concrete deep beams using nonlinear analysis. By using a sophisticated nonlinear finite element analysis program, the accuracy and objectivity of the assessment process can be enhanced. A computer program, the RCAHEST (Reinforced Concrete Analysis in Higher Evaluation System Technology), was used for the analysis of reinforced concrete structures. Tensile, compressive and shear models of cracked concrete and models of reinforcing and prestressing steel were used to account for the material nonlinearity of prestressed concrete. The smeared crack approach was incorporated. A bonded or unbonded prestressing bar element is used based on the finite element method, which can represent the interaction between the prestressing bars and concrete of a prestressed concrete member. The proposed numerical method for the evaluation of behavior and strength of prestressed concrete deep beams is verified by comparing its results with reliable experimental results.

Keywords: prestressed concrete; deep beams; nonlinear analysis; material nonlinearity; bonded or unbonded prestressing bar element.

1. Introduction

When the clean span-to-depth ratio of simply supported beams is less than 4, and they are loaded on one face and directly supported on the opposite face, it is customary to define these members as deep beams. Their capacity in either flexure or shear heavily depends on the detailing of loading and support. Deep beams shall be designed using either nonlinear analysis or strut-and-tie models (CSA 1994, *fib* 1999, MLTM 2007, ACI 2008).

To date, many studies have been conducted on the behavior and design of simply supported and continuous reinforced concrete deep beams (Pimentel *et al.* 2008, Lu *et al.* 2010). However, prestressed concrete deep beams have not been studied in any great detail (Alshegeir and Ramirez 1992, Tan and Mansur 1992, Tan *et al.* 1999).

Currently, there is no code provision for the design of prestressed concrete deep beams. The code does not give clear guidelines on how to apply a method to the design of prestressed concrete deep beams. There are only a few strut-and-tie models that are applicable for pretensioned and posttensioned deep beams (Tan and Mansur 1992, Ramirez 1994).

* Corresponding author, Professor, E-mail: hmshin@skku.edu

Strut-and-tie models can be formulated from experimental observations using failure crack patterns, recorded strains in the concrete and reinforcement, actual specimen detailing, and loading and support conditions. In design, much of this information is not readily available. For straight forward designs, an experienced engineer is generally capable of developing strut-and-tie models based on common engineering sense and knowledge of the behavior of structural concrete. However, in more complex design situations this practical knowledge is often not enough to develop safe and efficient strut-and-tie models. The development of a strut-and-tie model for a given situation is an iterative process because the widths of the struts and the size of the nodes depend on the forces in the struts and ties.

The primary objective of this study was to evaluate the behavior and strength of prestressed concrete deep beams using nonlinear finite element analysis. The finite element method is the most powerful tool in the numerical analysis of prestressed concrete deep beams. The nonlinear finite element analysis approach is used to illustrate the effects of prestressing, concrete compressive strength, and reinforcement detailing on the behavior and strength of these members.

An evaluation method for the behavior and strength of prestressed concrete deep beams is proposed. The proposed method uses a nonlinear finite element analysis program (RCAHEST, Reinforced Concrete Analysis in Higher Evaluation System Technology) developed by the authors (Kim and Shin 2001, Kim *et al.* 2003, Kim *et al.* 2005, Kim *et al.* 2007, Kim *et al.* 2009). A modified bonded or unbonded prestressing bars element is incorporated into the structural element library for RCAHEST so that it can be used to predict the inelastic behaviors of prestressed concrete deep beams.

2. Behavior and strength of prestressed concrete deep beams

The presence of prestressing in deep members contributes to delay inclined web-cracking, but it is not necessarily the critical factor in the inclination of the failure diagonal crack. The failure inclined crack for deep members will span between the point load and the support reaction. Flexure-shear-type cracking will seldom control the failure of this type of member. This general improvement in diagonal cracking strength and serviceability can be attributed to prestressing. It is envisaged that prestressing would delay flexural-shear cracking and result in higher shear capacity of the concrete member (Alshegeir and Ramirez 1992, Tan and Mansur 1992, Tan *et al.* 1999).

The behavior of prestressed concrete deep beams can be idealized as a strut-and-tie model, where the main steel and prestressed strands are represented by a tie and the force path in between the loading and support points are represented as an inclined strut. In deep beams, the ultimate capacity in either flexure or shear depends on the strength of the main diagonal strut and the appropriate detailing of the loading and support regions. The bearing plates determine one of the dimensions of the nodal zones under the load and at the support, thus affecting the state of stress at the node.

The strut-and-tie model assumes that the main reinforcement acts as a horizontal tension member while the concrete acts as inclined compressive struts to form a truss with nodes at concentrated loads and reactions. The strut-and-tie models adopted for the evaluation of the ultimate strength of deep beams are shown in Fig. 1 (Tan and Mansur 1992). If bearing failure is excluded, the member will fail either by the yielding of the tie or by crushing of one of the struts.

For deep beams without web reinforcement, the strut-and-tie model shown in Fig. 1 gives the strength as the smallest of the following three values

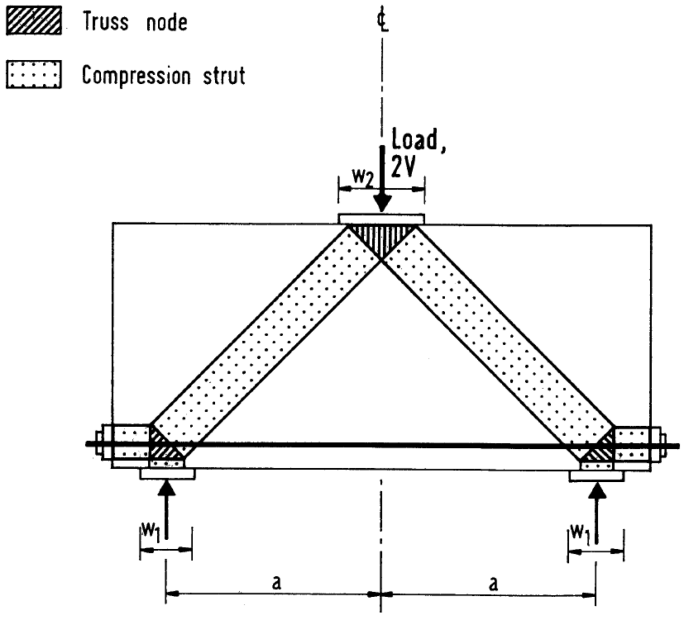

Fig. 1 Strut-and-tie model for prestressed concrete deep beams (Tan and Mansur 1992)

$$V_u = \frac{bw_1 f_c'}{1+\left(\frac{a}{d}+\frac{w_1}{2d}\right)^2} \tag{1}$$

$$V_u = 0.5bw_2 f_c' \tag{2}$$

$$V_u = (A_s f_y + A_{ps} f_{ps})\left(\frac{d}{a} - \frac{(A_s f_y + A_{ps} f_{ps})}{2f_c' ba}\right) \tag{3}$$

where V_u = ultimate shear capacity; b = deep beam width; w_1, w_2 = widths of bearing plates at the reactions and loading point; f_c' = concrete cylinder compressive strength; a = shear span; d = effective depth; A_s = areas of nonprestressed reinforcement; f_y = yield strength of nonprestressed reinforcement; A_{ps} = areas of prestressed reinforcement; f_{ps} = yield strength nonprestressed reinforcement.

Eqs. (1) and (2) correspond to the strength of the compressive struts as limited by the widths of the bearing plates at the reactions and load point, respectively, while Eq. (3) corresponds to the yielding of the tension tie (Tan and Mansur 1992).

3. Nonlinear finite element analysis program RCAHEST

RCAHEST is a nonlinear finite element analysis program used for analyzing reinforced concrete structures. The program was developed by Kim and Shin (2001), at the Department of Civil and Environmental Engineering, Sungkyunkwan University. The goal of the development is to apply a program for the modeling of various concrete structures under a variety of loading conditions.

3.1 General

The structural element library, RCAHEST is built around the finite element analysis program shell named FEAP, developed by Taylor (2000). FEAP is characterized by modular architecture and by the facility that allows the introduction of various types of custom elements, input utilities, and custom strategies and procedures.

The elements developed for the nonlinear finite element analyses of reinforced concrete bridge columns were the reinforced concrete plane stress element, the interface element and the lap spliced bar element (Kim *et al.* 2003, Kim *et al.* 2005, Kim *et al.* 2007, Kim *et al.* 2009). The material models described in the following sections were used as stress-strain relations at the Gauss integration points of each element. The elements were formulated by coordinate transformation from the element coordinate system to the reference coordinate system.

Accompanying the present study, the authors attempt to implement such a reinforced concrete plane stress element and a bonded or unbonded prestressing bar element as shown in Fig. 2.

3.2 Nonlinear material model for prestressed concrete

The nonlinear material model for the prestressed concrete is comprised of models to characterize the behavior of the concrete, in addition to models for characterizing the reinforcing bars and

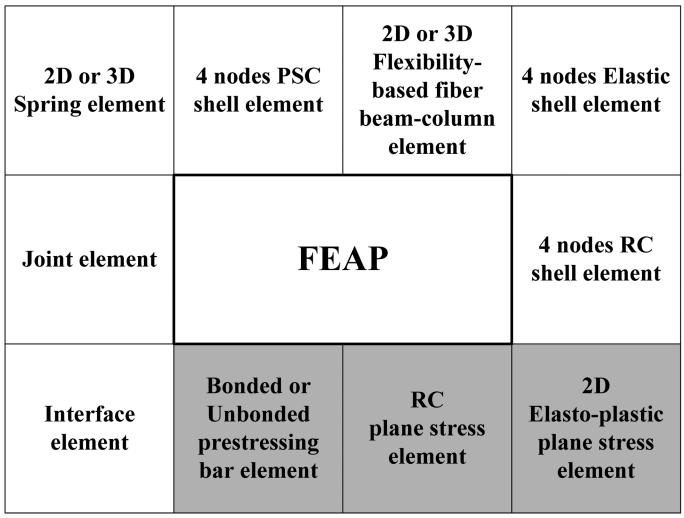

Fig. 2 Nonlinear finite element analysis program RCAHEST

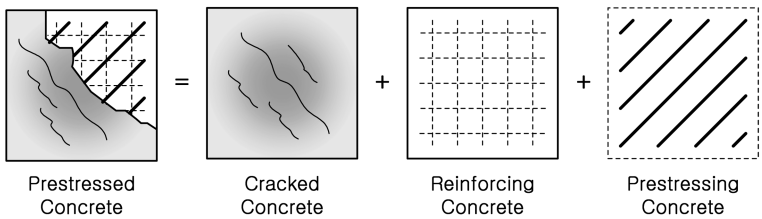

Fig. 3 Nonlinear material model for prestressed concrete

tendons (see Fig. 3). Models for concrete can be divided into models for uncracked concrete and cracked concrete. The basic model adopted for crack representation is a non-orthogonal fixed-crack method of the smeared crack concept, which is widely known to be a model for crack representation.

This section includes summaries of the material model used in the analysis. A full description of the nonlinear material model for reinforced concrete is provided by the authors in previous documents (Kim *et al.* 2003, Kim *et al.* 2005, Kim *et al.* 2007, Kim *et al.* 2009).

The elasto-plastic and fracture model for the biaxial state of stress proposed by Maekawa and Okamura (1983) is used as the constitutive equation for the uncracked concrete. For uncracked concrete, the nonlinearity, anisotropy, and strain softening effects are expressed independently of the loading history (Maekawa *et al.* 2001).

For cracked concrete, the three models are used for depicting the behavior of concrete in the direction normal to the crack plane, in the direction of the crack plane, and in the shear direction at the crack plane (see Fig. 4).

A refined tension stiffening model is obtained by transforming the tensile stress of concrete into the component normal to the crack. Using this approach, an improved accuracy is expected, especially when the reinforcing ratios in orthogonal directions are significantly different and when the reinforcing bars are distributed in only one direction. A modified elasto-plastic fracture model is used to describe the compressive behavior of concrete struts between cracks in the direction of the crack plane. The model describes the degradation in compressive stiffness by modifying the fracture parameter in terms of the strain perpendicular to the crack plane. The shear transfer model based on the contact surface density function (Li and Maekawa 1988) is used to consider the effect of shear stress transfer caused by the aggregate interlock at the crack surface. The contact surface is assumed to respond elasto-plastically, and the model is applicable to any arbitrary loading history.

The stress acting on a reinforcing bar embedded in concrete is not uniform and the stress value is the maximum at locations where the bar is exposed to a crack plane. The constitutive equations for

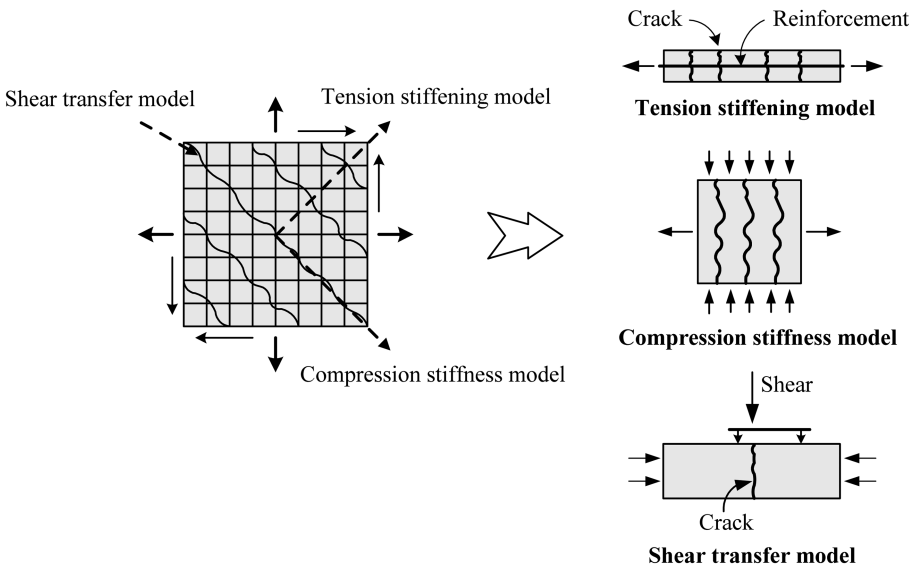

Fig. 4 Construction of cracked concrete model

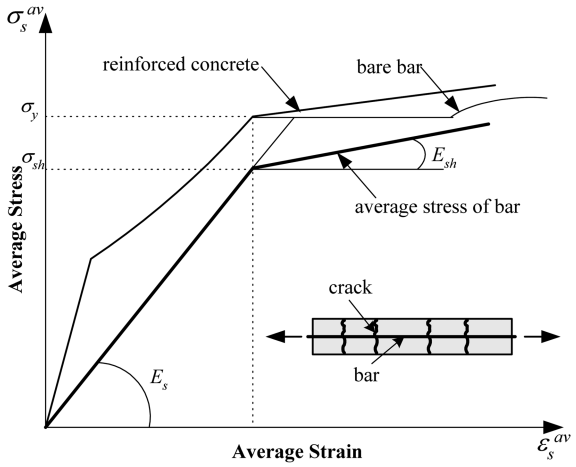

Fig. 5 Model for reinforcing bar in concrete

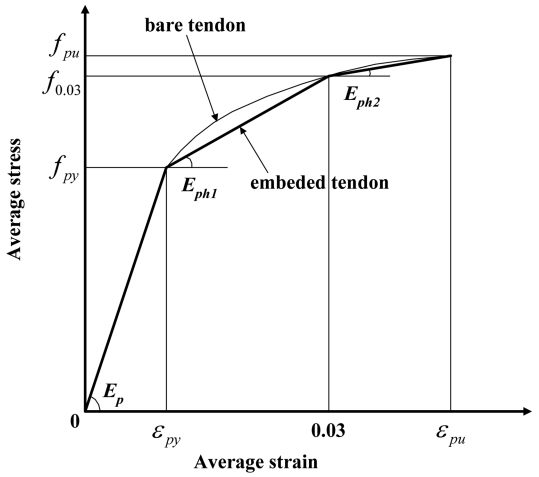

Fig. 6 Model for prestressing bars

the bare bar may be used if the stress strain relation is in the elastic range. The post-yield constitutive law for the reinforcing bar in concrete considers the bond characteristics, and the model is a bilinear model, as shown in Fig. 5.

Bilinear diagrams that are used to characterize the mild steel behavior of brusque yielding cannot be immediately extrapolated to a prestressing bar. For prestressing bars that do not have a definite yield point, a multilinear approximation may be required. In this study, the modified modeling is adopted for the present formulation as follows (see Fig. 6). A trilinear model for the stress-strain relationship of prestressing bars considering the bond effect has been used.

$$f_{pt} = E_p \varepsilon_p \quad \text{for} \quad \varepsilon_p < \varepsilon_{py} \tag{4}$$

$$f_{pt} = f_{py} + E_{ph1}(\varepsilon_p - \varepsilon_{py}) \quad \text{for} \quad \varepsilon_{py} \le \varepsilon_p < 0.03 \tag{5}$$

$$f_{pt} = f_{0.03} + E_{ph2}(\varepsilon_p - 0.03) \quad \text{for} \quad 0.03 \le \varepsilon_p < \varepsilon_{pu} \tag{6}$$

where f_{pt} = stress of prestressing bars; f_{py} = yielding strength of prestressing bars; f_{pu} = ultimate strength of prestressing bars; ε_p = strain of prestressing bars; ε_{py} = yielding strain of prestressing bars; ε_{pu} = ultimate strain of prestressing bars; E_p = Initial stiffness of prestressing bars; and E_{ph1}, E_{ph2} = strain hardening rates of the prestressing bars embedded in concrete.

3.3 Model for bonded or unbonded prestressing bars

An essential feature built into the program was the modeling of bonded or unbonded prestressing bars behavior. The modeling is based on the analysis method for reinforced concrete bridge piers with unbonded reinforcing or prestressing bars as proposed by Kim *et al.* (2008).

This method is similar to that for bonded bars, but the stress in the unbonded bars cannot be evaluated from force equilibrium and strain compatibility alone, since the assumption of a prefect bond between the bars and the concrete is no longer valid along the unbonded regions. Instead, the change in strain in the unbonded bars for any given loading depends on the average change in strain in the adjacent concrete over the entire unbonded length of the bars.

The strain in unbonded bars is not compatible with that of the adjacent concrete over the

unbonded length l_u. The average increase in strain in this unbonded bar, along its unbonded length, is then

$$\Delta\varepsilon_s = \frac{\Delta l_s}{l_u} \tag{7}$$

where Δl_s = total elongation of the unbonded bars.

The total strain ε_s is determined by

$$\varepsilon_s = \varepsilon_{pe} + \Delta\varepsilon_s \tag{8}$$

wher ε_{pe} = effective pre-strain in the unbonded bars.

The corresponding stress in the unbonded bars is obtained from the stress-strain curve in the previous section, whereas the stress in the bonded bars is obtained by the conventional strain compatibility method.

A highly iterative procedure is required to analyze the regions of unbonded bars. The analysis of unbonded bars was also found to be susceptible to convergence problems and some considerable effort was spent in developing program methodologies to provide efficient solutions. In this study, the matrix can be determined so as to make the convergence most effectively.

4. Numerical examples

4.1 Verification of the RCAHEST for deep beams

Data for the reinforced concrete deep beams obtained by Smith and Vantsiotis (1982) were used to verify the RCAHEST for deep beams. Analytical predictions were compared with measured results from four deep beams specimens tested.

Each beam was loaded directly on the top compression face with two equal concentrated loads 102 mm from the midspan and supported at the bottom (see Fig. 7). Bearing plates of 102×102×25 mm were used at the supports and the two points of loading. Physical properties of all beams tested are shown in Table 1.

Fig. 8 shows the finite element discretization and the boundary conditions for a sample of specimens, and the finite element model consists of eight-noded plane stress elements. In this

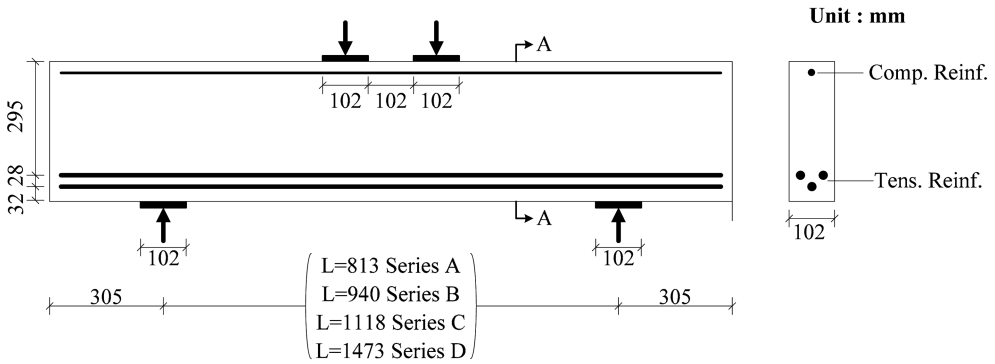

Fig. 7 Details of test specimens and setup (Smith and Vantsiotis 1982)

Table 1 Test specimens (Smith and Vantsiotis 1982)

Specimen		0A0-48	0B0-49	0C0-50	0D0-47
a/d		0.77	1.01	1.34	2.01
f_c' (MPa)		20.9	21.7	20.7	19.5
Tensile reinforcement	Bar size	#5			
	f_y (MPa)	421.5			
Compression reinforcement	Bar size	#2			
	f_y (MPa)	437.4			
Vertical and horizontal web reinforcement		-			

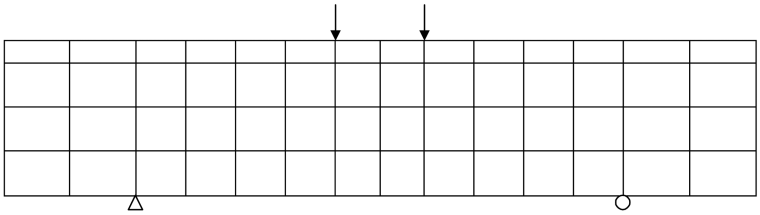

8-node RC element	48
8-node Elastic element	8

Fig. 8 Finite element mesh for reinforced concrete deep beams

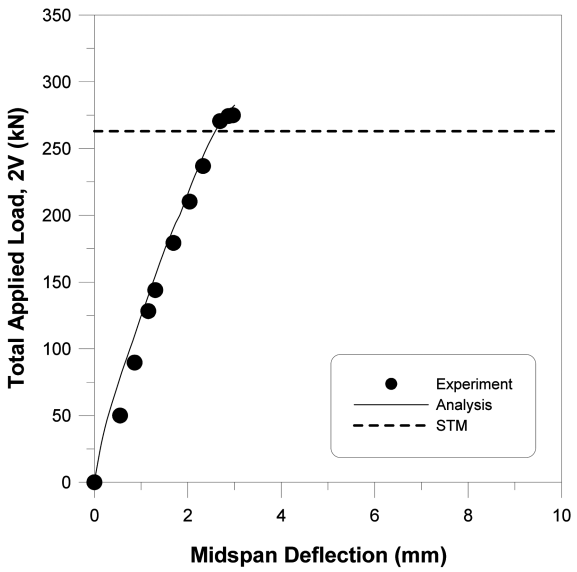

Fig. 9 Load-versus-deflection relationship for specimen 0A0-48

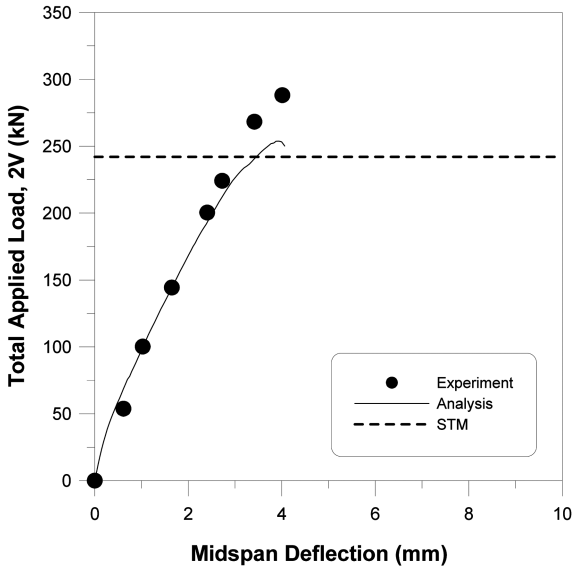

Fig. 10 Load-versus-deflection relationship for specimen 0B0-49

specimen series, the load was proportionally increased until failure occurred.

The total applied load versus midspan deflection curves for deep beams are shown in Figs. 9 through Fig. 12. Figs. 9 through 12 also show the ultimate shear strength of the reinforced concrete

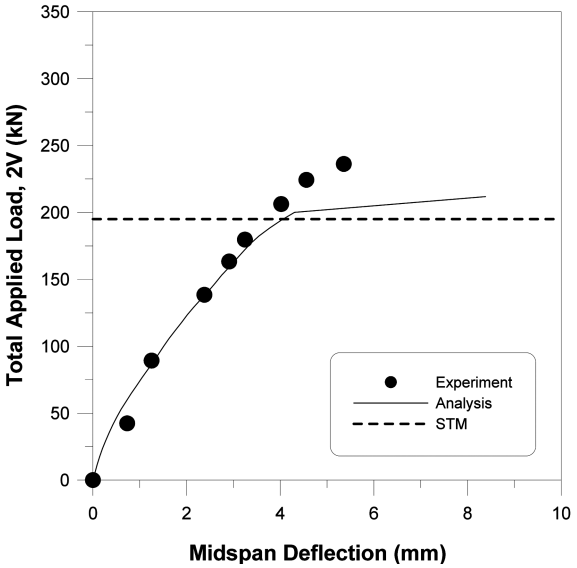

Fig. 11 Load-versus-deflection relationship for specimen 0C0-50

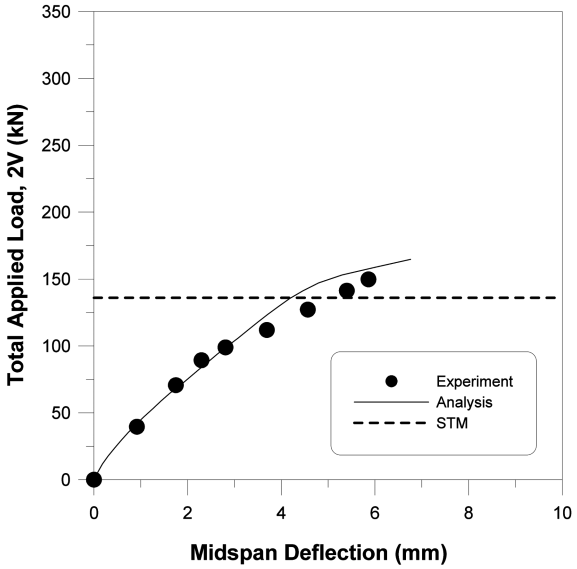

Fig. 12 Load-versus-deflection relationship for specimen 0D0-47

Table 2 Experiment and analysis results

Specimen	Mode of failure		V_u (kN)				
	Experiment	Analysis	Experiment (1)	Analysis (2)	STM (3)	(1)/(2)	(1)/(3)
0A0-48	Shear	Shear	272	283	263	0.96	1.04
0B0-49	Shear	Shear	298	259	242	1.15	1.23
0C0-50	Shear	Shear	231	212	195	1.09	1.18
0D0-47	Shear	Shear	147	141	136	1.04	1.08
Mean						1.06	1.13
COV						0.07	0.08

deep beams. The ultimate shear capacity is obtained from the strut-and-tie model (STM). The analytical results show reasonable concurrence with the experimental results.

The values given by all specimens were similar to the analytical results; comparative data are summarized in Table 2. In predicting the results of the series, under a variety of shear span-depth ratios (*a/d*), the mean ratios of experimental-to-analytical maximum strength were 1.06 at a COV of 7%. On the other hand, the strut-and-tie model gives an average ratio of test to predicted values of 1.13, with a COV of 8%. This shows that the predictions are consistent for reinforced concrete deep beams.

4.2 Application of the RCAHEST for prestressed concrete deep beams

The data for the prestressed concrete deep beams obtained by Tan and Mansur (1992) were used to verify the applicability of the proposed method. Analytical predictions were compared with measured results from four deep beams specimens tested.

Table 3 Test specimens (Tan and Mansur 1992)

Specimen		S14	S24	S34	S44
PPR*		0	0.33	0.67	1.00
Degree of prestress**		0	0.220	0.483	0.685
f_{cu} (MPa)		38.3	87.4	65.1	68.8
Prestressing wires	f_{py} (MPa)	1480			
	f_{pu} (MPa)	1623			
	E_{ps} (MPa)	193500			
Reinforcement	f_y (MPa)	508			

$$*\frac{A_{ps}f_{py}}{A_{ps}f_{py}+A_sf_y}$$

$$**\frac{A_{ps}f_{pe}}{A_{ps}f_{py}+A_sf_y}$$

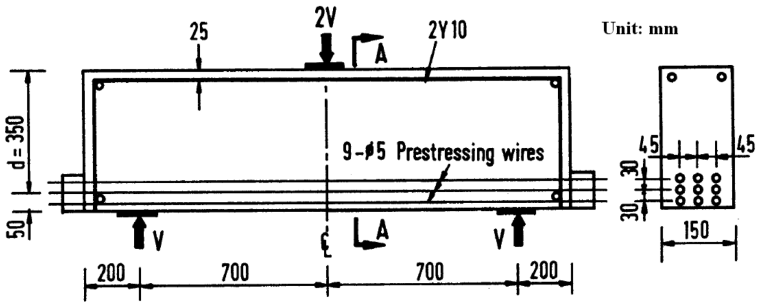

Fig. 13 Details of test specimens and setup (Tan and Mansur 1992)

4.2.1 Description of test specimens

A total of four test specimens were prepared and tested (see Table 3). For the deep beams, the overall depth was 400 mm, as shown in Fig. 13. Each specimen was made with an extra length of 200 mm at either end. In particular, this was partly to provide for the transmission length required for the transfer of prestress to the concrete in the pretensioned specimens.

For each specimen, the primary reinforcement consisted of nine prestressing wires, each 5 mm in diameter, placed symmetrically about a vertical axis through the midwidth of the cross section and at spacings of 45 and 30 mm in the transverse and vertical directions, respectively. The concrete cover to the centroid of the group of 9 wires was 50 mm; thus the tension steel ratio was 0.00337. Note that both the prestressed and nonprestressed reinforcement were made of the same prestressing wires and had the same yield strength (i.e. $f_y = f_{py}$).

All the specimens were simply supported and loaded through at the midspan, as shown in Fig. 13. Bearing plates measuring mm were used at the supports for all specimens and also at the loading point.

Each specimen was instrumented to measure the mid-span deflection and strains in both the prestressed and nonprestressed tension reinforcement.

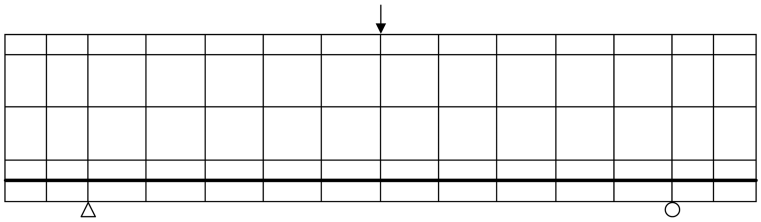

8-node RC element	**50**
8-node Elastic element	**6**
n-node Bonded prestressing bar element	**1**

Fig. 14 Finite element mesh for prestressed concrete deep beams

4.2.2 Description of analytical model

Fig. 14 shows the finite element discretization and the boundary conditions for a sample of specimens, and the finite element model consists of eight-noded plane stress elements. The bonded prestressing bar element was also used to represent the interaction between the prestressing bars and concrete of a prestressed concrete member. The concentrated loads were applied at the top surface, and the supports were represented by restrained nodes at the corresponding locations. In this specimen series, the load was proportionally increased until failure occurred.

4.2.3 Comparison with experimental results

The load-versus-deflection relationships for specimens are shown in Figs. 15 through Fig. 18. Figs. 15 through 18 also show the ultimate shear strength of the prestressed concrete deep beams.

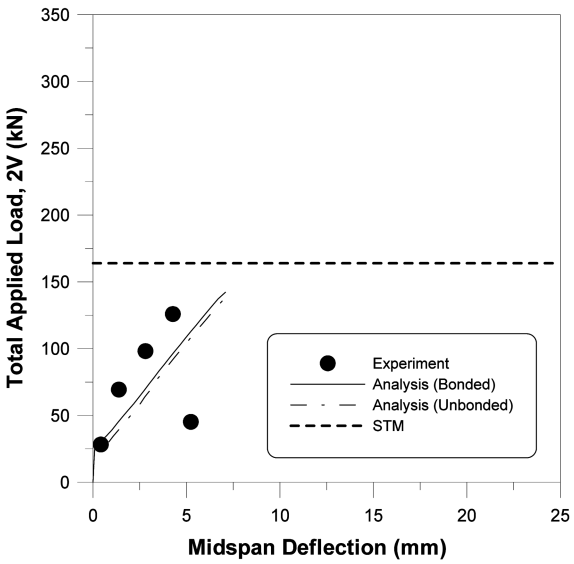

Fig. 15 Load-versus-deflection relationship for specimen S14

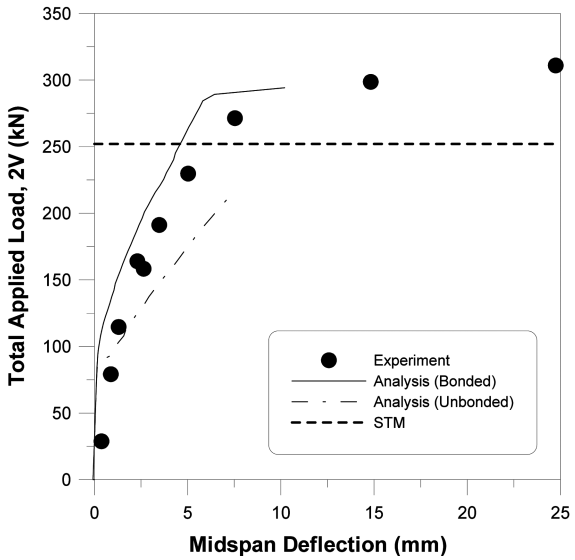

Fig. 16 Load-versus-deflection relationship for specimen S24

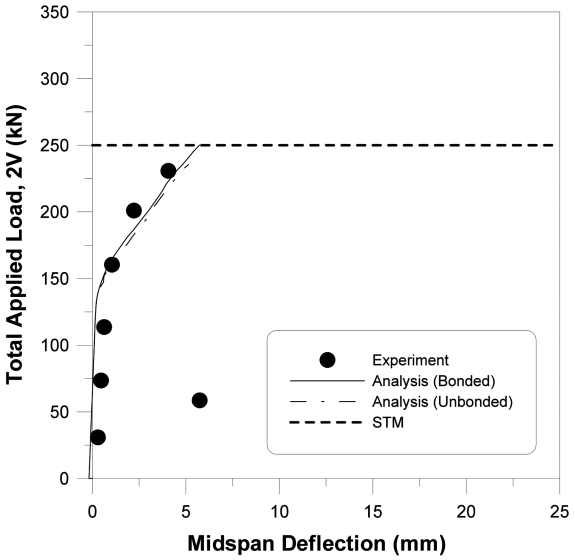

Fig. 17 Load-versus-deflection relationship for specimen S34

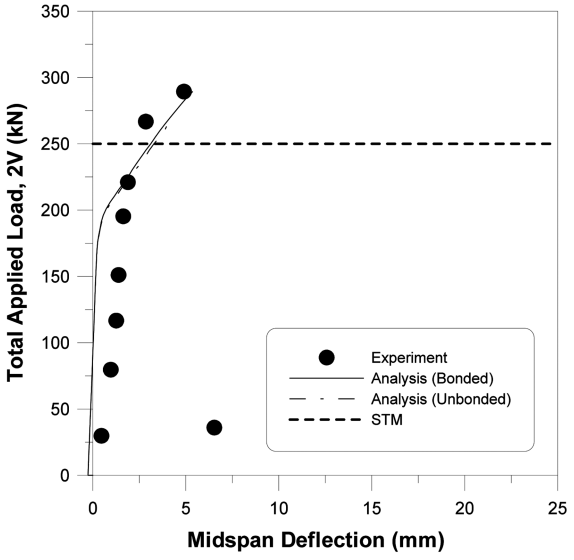

Fig. 18 Load-versus-deflection relationship for specimen S44

The ultimate shear capacity was obtained from the strut-and-tie model (STM) proposed by Tan and Mansur (1992).

Additionally, Figs. 15 to 18 show the analytical results in this study for the bonded and unbonded prestressing bars. For all specimens, good agreement is in load-deflection relation prior to cracking load. After cracking, the analytical results with unbonded tendons exhibit larger deflection under same load and have slightly lower ultimate strength than with bonded tendons. Because unbonded tendons can slip along the surrounding concrete, their contributions to stiffness and restraint to growth of crack are smaller than those of bonded tendons in specimens.

The analytical results show reasonable correspondence with the experimental results. For each of the test deep beams, the predicted and the measured maximum loads were in good agreement.

Specimens with higher degrees of prestress generally had greater stiffness. Upon first crack, specimen stiffness began to decrease, and this continued as more cracks developed. In cases where

Table 4 Experiment and analysis results

Specimen	Mode of failure		V_u (kN)				
	Experiment	Analysis	Experiment (1)	Analysis (2)	STM (3)	(1)/(2)	(1)/(3)
S14	Shear-compression	Shear-compression	62	71	82	0.87	0.76
S24	Flexure	Flexure	156	147	126	1.06	1.24
S34	Shear-compression	Shear-compression	115	125	125	0.92	0.92
S44	Shear-compression	Shear-compression	144	145	125	0.99	1.15
Mean						0.96	1.02
COV						0.09	0.22

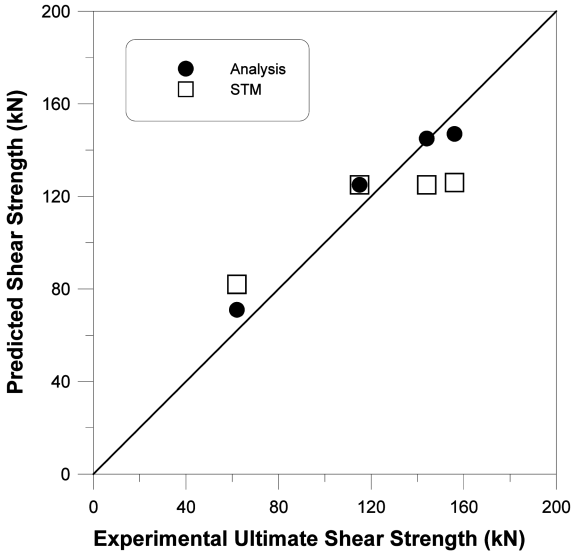

Fig. 19 Ultimate strength predictions for specimens

the specimen failed in shear-compression, the load decreased abruptly upon reaching the ultimate value and failure was brittle. On the other hand, for specimens that failed in flexure, the load remained almost constant with increasing deflection at ultimate, indicating ductile specimen behavior.

The values given by all specimens were similar to the analytical results; comparative data are summarized on Table 4. In predicting the results of the series, under a variety of degrees of prestress, the mean ratios of experimental-to-analytical maximum strength were 0.96 at a COV of 9%. On the other hand, the strut-and-tie model gives an average ratio of test to predicted values of 1.02, with a COV of 22%.

The variations of the strength are shown in Fig. 19 where the experimental and analytical results agree reasonably well. This shows that the predictions are consistent for prestressed concrete deep beams with different geometrical properties, prestressing, and web reinforcement configurations.

Fig. 20 shows the crack pattern for a sample of specimens at failure and the failure modes are summarized in Table 4. Fig. 20 also shows the predicted damage, and appears to be reasonable with respect to test observations.

In all specimens, the cracks propagated towards the loading point as the load was increased. This was accompanied by more flexural-shear cracks along the specimen shear spans, but there were relatively few such cracks in Specimen S24, which failed in flexure. Where the specimen failed in flexure, the failure was gradual and the specimen exhibited considerable ductility at ultimate.

Specimens that did not fail in flexure also experienced diagonal splitting, which eventually led to a shear-compression failure resulting in the crushing of concrete in the compression zone of deep beams. The failure of specimens was sudden and explosive. The specimens failed in either shear-compression or flexure, with the mode of failure changing from the former to the latter as the degree of prestress increased. The predictions of the failure modes of all the beams agree with the experimental results.

Figs. 21 and 22 show the typical measured and predicted steel strains in the tension reinforcement

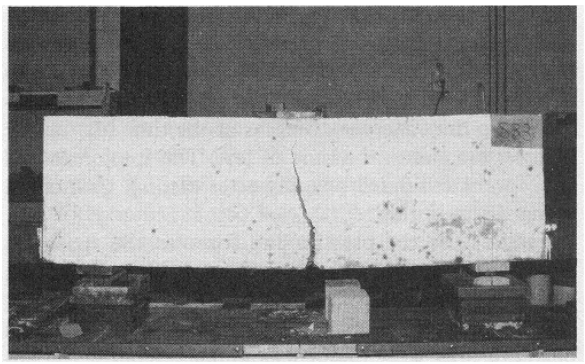

(a)

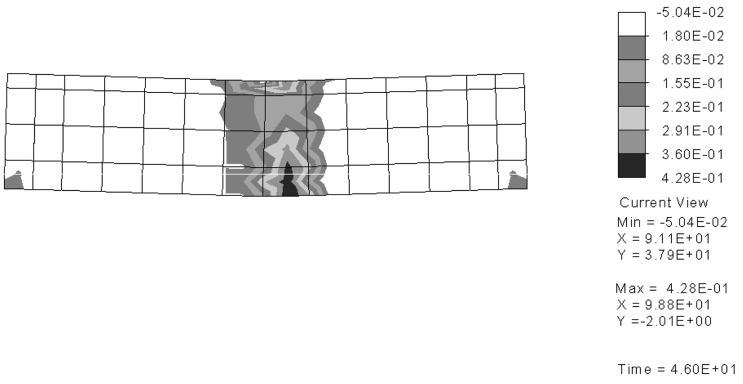

(b)

Fig. 20 Failure pattern for specimen S24: (a) experiment and (b) analysis

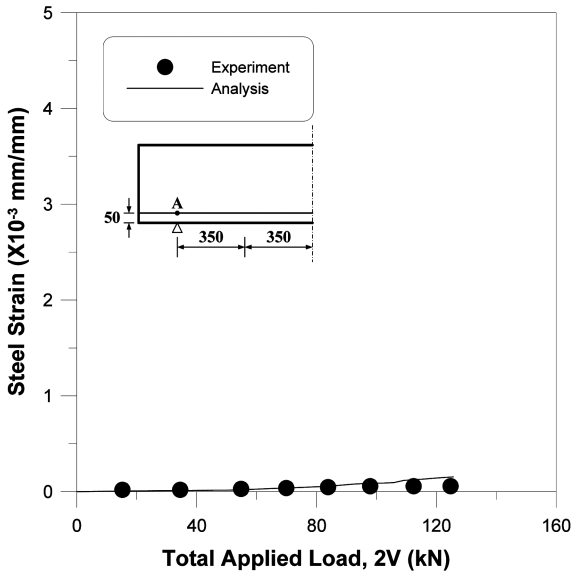

Fig. 21 Steel strain at location A for specimen S14

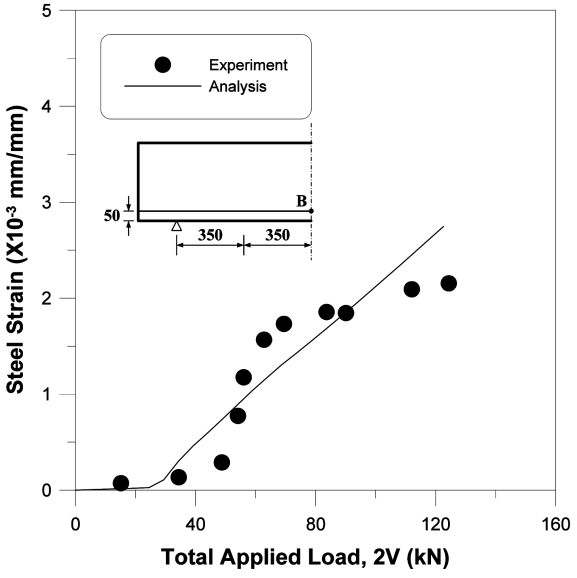

Fig. 22 Steel strain at location B for specimen S14

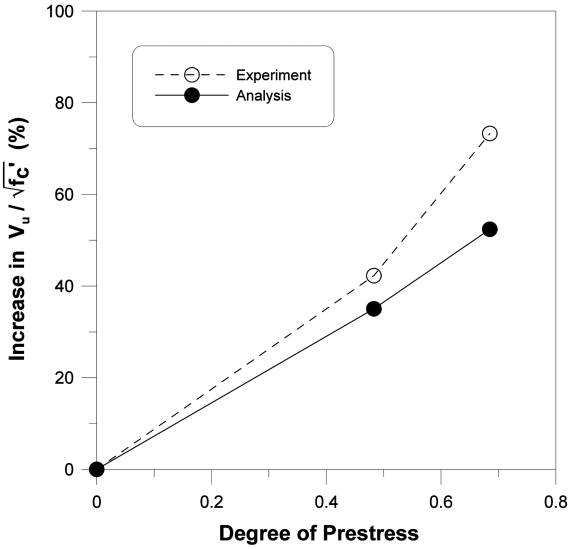

Fig. 23 Increase in $V_u/\sqrt{f_c'}$ due to prestress

for prestressed concrete deep beam specimens failing in shear-compression. The increase in steel strains at all locations due to the applied load was negligible at the initial stage. The steel strains increased significantly when the cracking loads were attained, particularly at locations at or near the cracks and in pretensioned specimens. The prestressing wires did not yield.

Fig. 23 shows the increase in the value of $v_u/\sqrt{f_c'}$ due to prestressing. Only the results of those specimens that failed in shear are included in the plot. The ultimate shear stress increases with an increase in the degree of prestress.

There are specimens (0C0-50, and S24) with some differences, which are caused by both experimental and analytical error. The failure modes are very brittle and it is difficult to determine the ultimate displacement for this mode from experiments. However, It is expected that by using the proposed method the evaluation of behavior and strength of prestressed concrete deep beams can be predicted accurately, and this enables more rational and reliable design of prestressed concrete deep beams.

5. Conclusions

In this study, an attempt was made to establish a framework for the evaluation of behavior and strength of prestressed concrete deep beams. Theory and formulations are described for analytical models to be implemented with numerical methods for predicting the behavior and strength of prestressed concrete deep beams. The agreement between the numerical simulations and experimental findings demonstrate the overall accuracy and reliability of the analytical models in predicting the response of prestressed concrete deep beams. Based on the results of the numerical simulations and comparisons with experimental data, the following conclusions were reached.

(a) The proposed constitutive model and numerical analysis describe with acceptable accuracy the inelastic behavior of the prestressed concrete deep beams. This method may be used for the nonlinear analysis and design of prestressed concrete deep beams.

(b) The results from the finite element simulation using the new model agree very well with the experimental observations, especially with regards to load-deflection response, crack patterns at different load stages, and failure modes.
(c) The ultimate shear capacity of prestressed concrete deep beams increases with an increasing degree of prestress and increasing concrete strength.
(d) Further efforts should be made to include certain procedures in the current design codes to direct the engineers toward an acceptable method for evaluating the available strength in existing prestressed concrete deep beams.
(e) Future work by the authors will include the formulation of a constitutive model for time-dependent effects such as concrete creep, shrinkage and relaxation of prestressing bars.

Acknowledgements

This research was supported by a grant (code#06-E01) from the Virtual Construction Research Center Program funded by the Ministry of Land, Transport and Maritime Affairs of the Korean government. The authors wish to express their gratitude for the support received.

References

Alshegeir, A. and Ramirez, J.A. (1992), "Strut-tie approach in prestensioned deep beams", *ACI Struct. J.*, **89**(3), 296-304.
American Concrete Institute (2008), *Building code requirements for structural concrete (ACI 318M-08) and commentary*, Farmington Hills, Michigan, USA.
Canadian Standards Association (1994), *Design of concrete structures: structures (Design) - a national strandard of Canada (CANA23.3-94)*, Rexdale, Ontario, Canada.
The International Federation for Structural Concrete (*fib*) (1999), *Structural concrete; textbook on behavior, design and performance updated knowledge of the CEB/FIP model code 1990 Volume 3*, The International Federation for Structural Concrete (*fib*), Lausanne, Switzerland.
Kim, T.H., Hong, H.K., Chung, Y.S. and Shin, H.M. (2009), "Seismic performance assessment of reinforced concrete bridge columns with lap splices using shaking table tests", *Mag. Concrete Res.*, **61**(9), 705-719.
Kim, T.H., Kim, Y.J. and Shin, H.M. (2007), "Seismic performance assessment of reinforced concrete bridge columns under variable axial load", *Mag. Concrete Res.*, **59**(2), 87-96.
Kim, T.H., Lee, K.M., Chung, Y.S. and Shin, H.M. (2005), "Seismic damage assessment of reinforced concrete bridge columns", *Eng. Struct.*, **27**(4), 576-592.
Kim, T.H., Lee, K.M., Yoon, C.Y. and Shin, H.M. (2003), "Inelastic behavior and ductility capacity of reinforced concrete bridge piers under earthquake. I: theory and formulation", *J. Struct. Eng. - ASCE*, **129**(9), 1199-1207.
Kim, T.H., Park, J.G, Kim, Y.J. and Shin, H.M. (2008), "A computational platform for seismic performance assessment of reinforced concrete bridge piers with unbonded reinforcing or prestressing bars", *Comput. Concrete*, **5**(2), 135-154.
Kim, T.H. and Shin, H.M. (2001), "Analytical approach to evaluate the inelastic behaviors of reinforced concrete structures under seismic loads", *J. Earthq. Eng. Soc. Korea, EESK*, **5**(2), 113-124.
Li, B. and Maekawa, K. (1988), "Contact density model for stress transfer across cracks in concrete", *Concrete Eng. JCI*, **26**(1), 123-137.
Lu, W.Y., Hwang, S.J. and Lin, I.J. (2010), "Deflection prediction for reinforced concrete deep beams", *Comput. Concrete*, **7**(1), 1-16.
Maekawa, K. and Okamura, H. (1983), "The deformational behavior and constitutive equation of concrete using elasto-plastic and fracture model", *J. Fac. Eng., Univ. Tokyo*, **37**(2), 253-328.

Maekawa, K., Pimanmas, A. and Okamura, H. (2001), *Nonlinear mechanics of reinforced concrete*, SPON Press.
Ministry of Land, Transport, and Maritime Affairs (2007), *Concrete structural design code*, MLTM, Korea.
Pimentel, M., Cachim, P. and Figueiras, J. (2008), "Deep-beams with indirect supports: numerical modeling and experimental assessment", *Comput. Concrete*, **5**(2), 117-134.
Ramirez, J.A. (1994), "Strut-tie design of prestensioned concrete members", *ACI Struct. J.*, **91**(4), 572-578.
Smith, K.N. and Vantsiotis, A.S. (1982), "Shear strength of deep beams", *ACI Struct. J.*, **79**(3), 201-213.
Tan, K.H., Lu, H.Y. and Teng, S. (1999), "Size effect in large prestressed concrete deep beams", *ACI Struct. J.*, **96**(6), 937-946.
Tan, K.H. and Mansur, M.A. (1992), "Partial prestressing in concrete corbels and deep beams", *ACI Struct. J.*, **89**(3), 251-262.
Taylor, R.L. (2000), *FEAP - a finite element analysis program,* Version 7.2 Users Manual, Volume 1 and Volume 2.

CC